UC Irvine
UC Irvine Previously Published Works

Title

Dynamics of Active Subglacial Lakes in Recovery Ice Stream

Permalink

https://escholarship.org/uc/item/8nb5g9kd

Journal

Journal of Geophysical Research Earth Surface, 123(4)

ISSN

2169-9003

Authors

Dow, CF
Werder, MA
Babonis, G
et al.

Publication Date

2018-04-01

DOI

10.1002/2017jf004409

Peer reviewed

Key Points:
- Basal hydrology model outputs demonstrate that regional ice stream hydrological characteristics drive subglacial lake drainage timing
- Simulations show pressure waves moving through Recovery Ice Stream that influence the rate of lake growth and drainage volume
- Modeled R-channel evolution indicates their persistence over multiple years after lake drainages, thus reducing the local water pressure

Supporting Information:
- Supporting Information S1
- Movie S1
- Movie S2

Correspondence to:
C. F. Dow,
christine.dow@uwaterloo.ca

Dynamics of Active Subglacial Lakes in Recovery Ice Stream

C. F. Dow[1,2] ⓘD, M. A. Werder[3] ⓘD, G. Babonis[4], S. Nowicki[2] ⓘD, R. T. Walker[2,5], B. Csatho[4] ⓘD, and M. Morlighem[6] ⓘD

[1]Department of Geography and Environmental Management, University of Waterloo, Waterloo, Ontario, Canada, [2]Cryospheric Sciences Laboratory, NASA Goddard Space Flight Center, Greenbelt, MD, USA, [3]Laboratory of Hydraulics, Hydrology and Glaciology (VAW), ETH Zurich, Zurich, Switzerland, [4]Geology Department, State University of New York at Buffalo, Buffalo, NY, USA, [5]Earth System Science Interdisciplinary Center, University of Maryland, College Park, MD, USA, [6]Department of Earth System Science, University of California, Irvine, CA, USA

Abstract Recovery Ice Stream has a substantial number of active subglacial lakes that are observed, with satellite altimetry, to grow and drain over multiple years. These lakes store and release water that could be important for controlling the velocity of the ice stream. We apply a subglacial hydrology model to analyze lake growth and drainage characteristics together with the simultaneous development of the ice stream hydrological network. Our outputs produce a good match between modeled lake location and those identified using satellite altimetry for many of the lakes. The modeled subglacial system demonstrates development of pressure waves that initiate at the ice stream neck and transit to within 100 km of the terminus. These waves alter the hydraulic potential of the ice stream and encourage growth and drainage of the subglacial lakes. Lake drainage can cause large R-channels to develop between basal overdeepenings that persist for multiple years. The pressure waves, along with lake growth and drainage rates, do not identically repeat over multiple years due to basal network development. This suggests that the subglacial hydrology of Recovery Ice Stream is influenced by regional drainage development on the scale of hundreds of kilometers rather than local conditions over tens of kilometers.

Plain Language Summary Ice streams are fast-flowing areas of the Antarctic ice sheet that drain large quantities of ice into the ocean, contributing to sea level rise. We have run a model of water flow underneath Recovery Ice Stream to examine lakes that build up and drain underneath kilometers of ice to find out whether they have an impact on the speed of the overlying ice. We find that the timing of the lake growth and drainage is determined by the hydrological conditions underneath the entirety of the ice stream, stretching over hundreds of kilometers. As the lakes drain, they melt channels that connect as sub-ice rivers between the drainage basins. We also find that the regions of highest water pressure, and therefore the fastest-moving overlying ice, are concentrated in the deepest parts of the trough that the ice stream flows through. This is an important finding for determining the controls on fast ice stream flow speed and therefore the stability of the Antarctic ice sheet.

1. Introduction

Subglacial hydrological systems of Antarctic ice streams are both spatially and temporally dynamic, including regions of active water flux (Siegfried et al., 2016) and areas of water storage in subglacial lakes (Fricker et al., 2016). The distribution and pressure of basal water is a direct control on ice stream flow speed (Joughin et al., 2002; Tulaczyk et al., 2000), and correspondingly, determining the characteristics and variability of hydrological networks is of great importance for predicting Antarctic mass change. The presence of subglacial lakes in Antarctica has been detected by both satellite altimetry and radar-based methods. In the interior of the ice sheet, these lakes appear to be deep and stable and are identified by bright flat reflectors in radar data (Siegert, 2005). In the dynamic ice streams, however, subglacial lakes are more active, with growth and drainage interpreted from satellite altimetry-derived ice surface uplift and subsidence over the range of 1–5 years (e.g., Fricker et al., 2010).

Antarctic subglacial lakes have been modeled within synthetic ice dynamics models (Pattyn, 2008; Sergienko et al., 2007) and as basins that are filled and drained by tuning with satellite altimetry data (Carter & Fricker, 2012; Carter et al., 2009, 2011). Recent work by Carter et al. (2017) suggests that Antarctic lake dynamics cannot

be influenced by the formation of Röthlisberger (R-) channels that melt upward into the ice, instead arguing that sediment canals are necessary to allow lake drainage. These treatments of Antarctic subglacial lakes are different from those models that examine ice marginal lake outburst floods or subglacial jökulhlaups, where rapid (on the scale of days to weeks) drainage occurs. Models examining the latter focus on the water pressure allowing ice uplift and downstream lake drainage (e.g., Ng & Liu, 2009; Nye, 1976) or negative pressure gradients that prevent outflow of the lakes until they are reversed by hydrological development (e.g., Evatt et al., 2006; Fowler, 1999; Kingslake, 2015). In contrast, the active Antarctic subglacial lakes differ because they drain over a time scale of years and can become much larger ($>10 \, km^2$), although often shallower (e.g., $<10 \, m$ deep) than ice marginal or jökulhlaup lakes. The work of Dow et al. (2016) found that at no time were hydraulic pressure gradients reversed when applying a synthetic hydrology model to Antarctic lakes. Instead, lake dynamics were driven by spatially and temporally varying conductivity of the basal drainage system including the growth of R-channels that drained the lake. The Dow et al. (2016) study applied a synthetic, planar topography with one overdeepening, designed to emulate Recovery Ice Stream. However, until now, a 2-D approach to catchment-scale hydrology modeling with Antarctic topography including multiple lake basins has not been attempted.

Recovery Ice Stream is one region with multiple (at least nine) active lakes that fill and drain in sequence over 2–4 years (Fricker et al., 2014). Recovery Ice Stream is located in Dronning Maud Land in East Antarctica, draining into the Filchner-Ronne Ice Shelf (Figure 1a). This ice stream drains a catchment of $5.4 \times 10^5 \, km^2$, equivalent to 8% of the East Antarctic Ice Sheet (Joughin et al., 2006). The average speed of the ice stream is $\sim$100 m/a with a maximum speed of 922 m/a, while the upper catchment area flows more slowly at a speed of $\sim$6 m/a (Rignot et al., 2011). Recovery Ice Stream flows through a deep trough with depths up to 2,700 m below sea level. The width of the ice stream is $\sim$55 km and the length $\sim$700 km. At the head of the ice stream, four additional large lakes (with a combined area of 13,300 km^2) have been discovered through radar analysis of basal reflectivity and flat ice surface topography (Bell et al., 2007; Langley et al., 2011, 2014). These large lakes appear to be more stable than the active downstream lakes.

Although the ice above the active Recovery lakes is known to uplift and subside in sequence (Fricker et al., 2014), implying downstream flow of subglacial water, there has yet to be a detailed hydrological analysis of the drivers of lake filling and drainage, the development of hydrological systems in the wider ice stream as a result of lake drainage, and the dynamic impact of these lakes on ice flow. Here we use the Glacier Drainage System model (GlaDs; Werder et al., 2013), a 2-D subglacial drainage model, to estimate Recovery Ice Stream basal hydrological development with emphasis on examining the lake characteristics. We advance from the Dow et al. (2016) study by including realistic ice stream topography and ice stream characteristics and compare outputs with ice surface altimetry data. Our aims are to establish (1) the controls that allow lakes to grow and drain, (2) whether lake growth and drainage rates are likely to be variable over time, (3) if R-channels are features that are likely to occur in this ice stream, and (4) identify the likely impacts of subglacial hydrological development on the ice flow dynamics of Recovery Ice Stream.

2. Methods

2.1. Model Setup

GlaDS is a subglacial hydrology model that includes equations for simultaneous development of a linked cavity system and R-channels in a 2-D finite element configuration. The distributed sheet on the elements and the channels on the element edges interact to replicate a coevolving subglacial system. Werder et al. (2013) fully described the model and Dow et al. (2016) discussed application of this model to Antarctic ice streams and subglacial lakes.

The number of nodes that can be included in the model domain for efficient running is $\sim$20,000 nodes and therefore it is not currently possible to adequately resolve both the full Recovery catchment and the ice stream. As a result, we ran a full catchment model with large element sizes ($>40 \, km^2$ area) and a domain length of 1,500 km to estimate the water flux rate into the neck of the ice stream trunk. We then reduced the model domain to a length of 720 km including the ice stream and its neck (Figure 1b), thus allowing greater refinement of our domain elements. We apply the catchment flux rate as a Neumann condition into the upper boundary. The modeled region is further refined to exclude nunataks, which cause model instability. Within the restricted domain, the maximum element edge is 9 km at the ice stream neck. In the overdeepened areas, where the lakes are forming, greater mesh refinement is applied and the edge lengths are reduced to a minimum of 500 m.
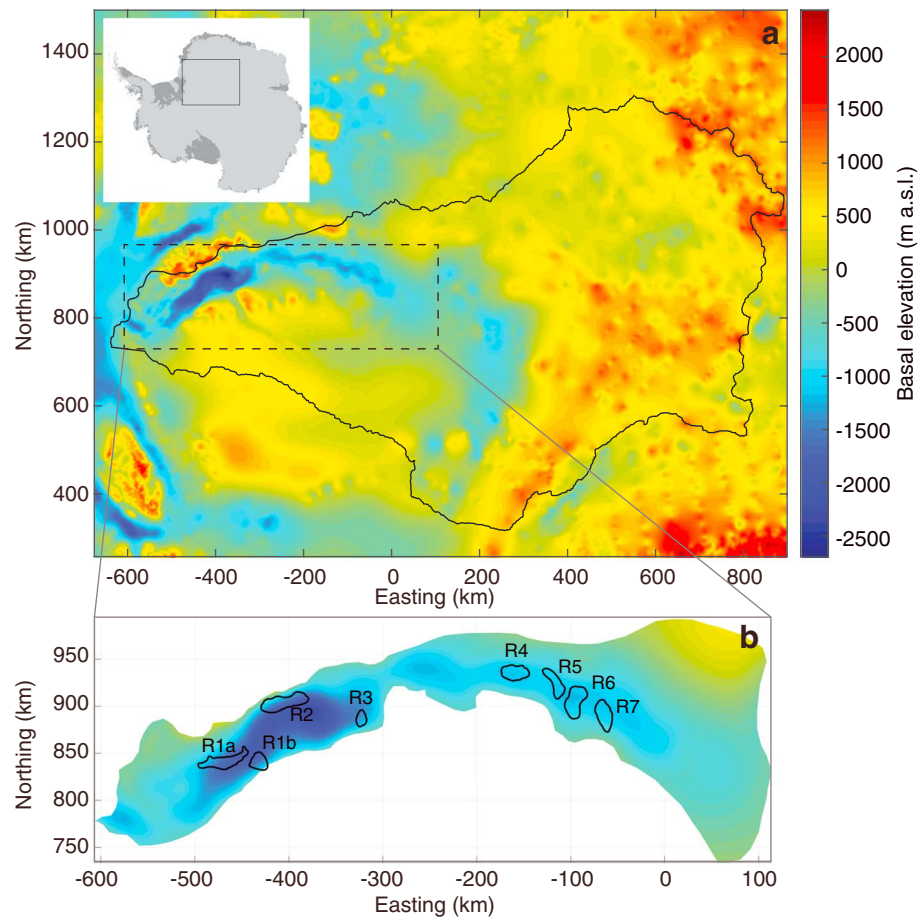
Figure 1. (a) Basal digital elevation model (nonsmoothed) of Recovery Ice Stream and its catchment (black line) including both BEDMAP2 data and the mass conservation data. (b) Modeling domain with smoothed basal topography and the locations of the Ice Cloud and land Elevation Satellite-derived lakes from Fricker et al. (2014). Inset shows the study location in Antarctica.

We use BEDMAP2 by Fretwell et al. (2013) for the Recovery catchment surface and basal digital elevation models (DEMs). However, the Recovery region is not well covered by flight lines (due to its extreme distance from research bases) and the topography therefore has associated errors. Within the Recovery Ice Stream, it is necessary that the most accurate topography is utilized to best replicate the lake dynamics. As a result, we have produced a more detailed basal topography using a mass conservation method (Morlighem et al., 2011). This method combines sparse radar-derived ice thickness measurements from the Center for Remote Sensing of Ice Sheets, velocity data from Rignot et al. (2011), and surface mass balance data from RACMO 2.3 (van Wessem et al., 2014). The bed topography is deduced by subtracting the modeled ice thickness from the BEDMAP2 surface DEM, and has a horizontal resolution of ∼300 m. This new topography increases the depth of Recovery Ice Stream bed from the BEDMAP2 level by 970 m and has greatly enhanced the resolution of the most active regions where subglacial lakes lie. Inland of the ice stream, the ice velocity is too slow for accurate mass conservation inversion methods. For GlaDS stability, we smooth the basal topography with a 9 km moving average filter to prevent jumps between the mass conservation and BEDMAP2 data sets; this length of filter was required due to the maximum element edge length at the ice stream neck. The resulting basal DEM is shown in Figure 1b.

Water is produced at the bed of Recovery catchment and ice stream through geothermal and frictional heating. This water is included in the model as a constant and uniform input across the domain. The initial input rate is 0.5 mm/a, which is likely too small for the Recovery region and is used to run the model to steady state (this lower input rate is necessary to prevent hydrological transience as discussed in Dow et al., 2016). From this state, water input is increased to the predicted Recovery water production rate of 1 mm/a

Table 1
Model Parameters

Parameter	Value	Unit
Bedrock bump height	0.1	m
Boundary input (mean)	$\sim 1 \times 10^{-4}$	m^2/s
Cavity spacing	2	m
Channel conductivity	5×10^{-2}	$m^{3/2} \cdot kg^{-1/2}$
Englacial void ratio	10^{-5}	
Glen's flow constant (n)	3	
Gravitational acceleration	9.81	m/s^2
Ice density	910	kg/m^3
Ice flow constant	2.5×10^{-25}	Pa^{-n}/s
Latent heat of fusion	3.34×10^5	J/kg
Sheet conductivity	1×10^{-3}	$m^{7/4} \cdot kg^{-1/2}$
Sheet input	1	mm/a
Sheet width below channel	2	m
Water density	1,000	kg/m^3

(Fricker et al., 2014) over 7 years. At the same time, the upper boundary flux is also added into the system over a 1 year ramp. Both the boundary flux and basal water are input only into the distributed system elements and not directly into channels. The model is initiated with no channels and their growth is instead driven by water flow in the distributed system. The lateral boundary has a Neumann condition set to zero inflow. The downstream boundary has a Dirichlet pressure condition set at a value representing average ice overburden pressure at the ocean terminus of Recovery Ice Stream.

Basal sliding for the Recovery Ice Stream is estimated as 90% of the observed surface ice velocities (Rignot et al., 2011). The basal sliding input into the model controls the cavity opening rate of the subglacial distributed hydrological system. Although the distributed portion of the model is set up to emulate a linked cavity system, the conductivity of sediment-based systems may behave in a similar manner (Creyts & Schoof, 2009). The standard inputs for our GlaDS runs are listed in Table 1 following Dow et al. (2016). We run the model from the steady state condition for a total of 33 years.

2.2. Ice Elevation Time Series

We use surface elevation data from the Geoscience Laser Altimeter System (GLAS) aboard NASA's Ice Cloud and land Elevation Satellite (ICESat), spanning a collection time period from 2003 to 2009. GLA05 Level-1B Global Waveform-based Range Corrections Data and GLA12 Level-2 Antarctic and Greenland Ice Sheet Altimetry Data, Release 633 data products were obtained from the National Snow and Ice Data Center. We applied the Gaussian-Centroid offset correction, derived from GLA05, to the GLA12 product following Borsa et al. (2014). We generate surface elevation time series using the Surface Elevation Reconstruction and Change detection (SERAC) method developed by Schenk and Csatho (2012), at ascending and descending ground track crossover locations in the study area. After identifying crossover locations, all elevation data within a surface patch of 1×1 km around each crossover location were used to determine the surface shape, as well as surface elevation changes through time for all available observation periods. The resulting time series were filtered by location to remove those above exposed rock outcrops. Parameters characterizing the ICESat waveform were examined to assess the precision of the elevation data. Poor-quality data, characterized by an apparent reflectivity of <0.1 or a waveform misfit of >0.035 volts were excluded from the SERAC processing, following the recommendation of Smith et al. (2009). We assume an accuracy of 0.05–0.2 m for single shots on land ice surfaces (Fricker et al., 2005).

3. Results

3.1. Lake Location

GlaDS produces multiple lakes within Recovery Ice Stream. We define a "lake" as any region where the water depth exceeds 20 cm over an area of >5 km^2 in order to differentiate from filled cavities. We follow the naming conventions for the Recovery Lakes of Fricker et al. (2014). As our model domain is restricted to a length
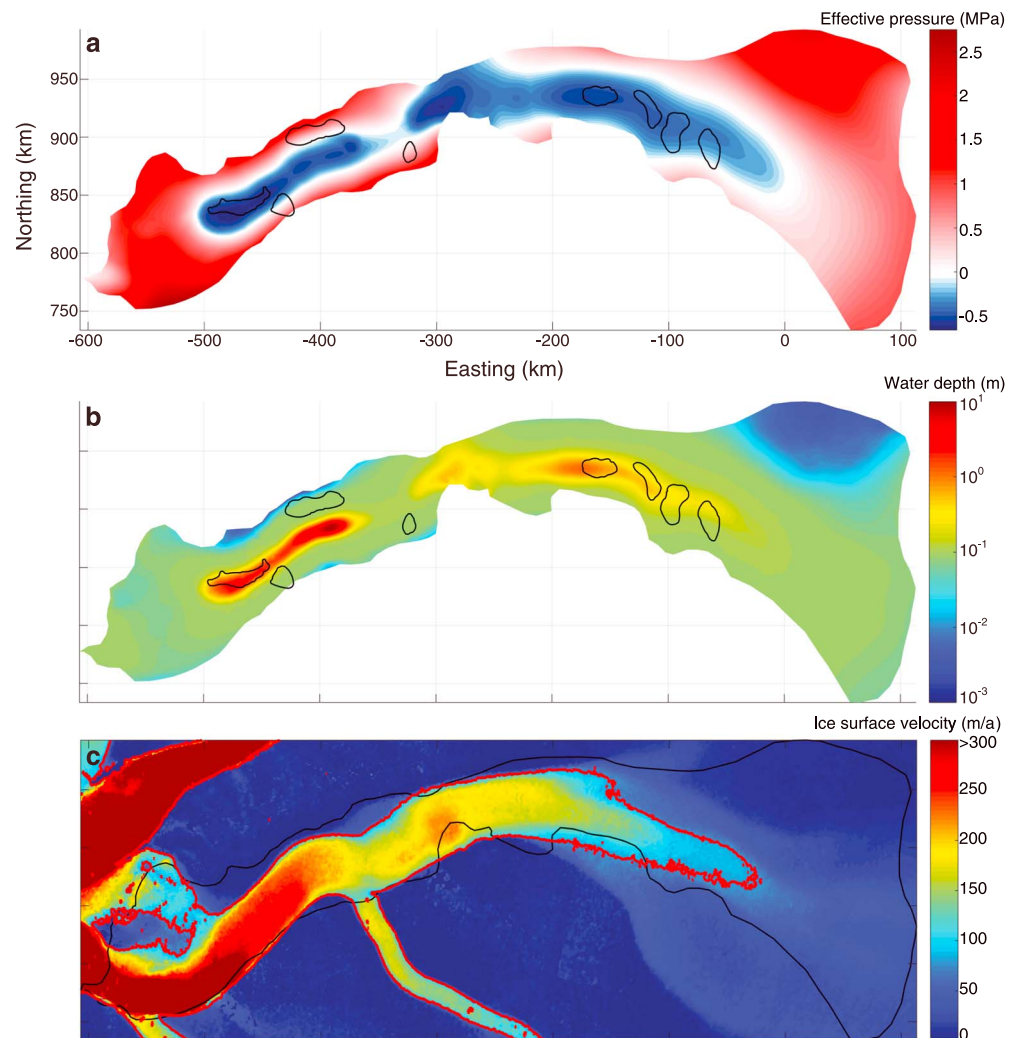
Figure 2. Recovery Ice Stream domain plots including, for the entire model run, (a) the minimum effective pressure in each element and (b) the maximum water depth in each element (note that outputs are on a log scale). Lakes identified from ICESat are delimited in black. (c) Recovery Ice Stream surface velocity (note that data are limited to 300 m/a for plotting clarity; Rignot et al., 2011). The model domain is outlined in black and the 80 m/a contour in red.

of 720 km, we have comparable results with Recovery 1 through 7 (referred to here as R1 through R7). Due to two separate lake signals that appear in our model outputs, we divide Recovery 1 into R1a and R1b (Figure 1b). There is good agreement between the lake locations predicted by the model and those observed from ice altimetry analysis (Figure 2b); we see lake growth in the same region as R1 and R4–R7 (Figure 3). We also see a strong lake signal in the vicinity where R2 is supposed to be located, as identified by ICESat altimetry data. However, our modeled lake is in the middle of the ice stream whereas R2 is toward the margin with an offset of 20 km. This is possibly due to limited data driving inversion for Recovery Ice Stream topography, and more basal topography data could correct this. Likely for similar reasons, we see no lake signal for the smaller R3 lake. Finally, the model produces an additional lake that forms 320 km from the terminus between R3 and R4 (Figure 2b).

3.2. Pressure Wave

The model outputs show two full ice stream lake growth and drainage cycles over the 33 year run period. Lake drainage generally follows a cascade pattern with upper lakes filling and draining prior to lakes downstream in the ice stream (Figure 3; also see Movies S1 and S2). This is a new output from this model configuration, as the synthetic experiments for Recovery Ice Stream using a simplified planar topography, discussed in Dow et al. (2016), only involved one overdeepening. In these synthetic experiments, it was found
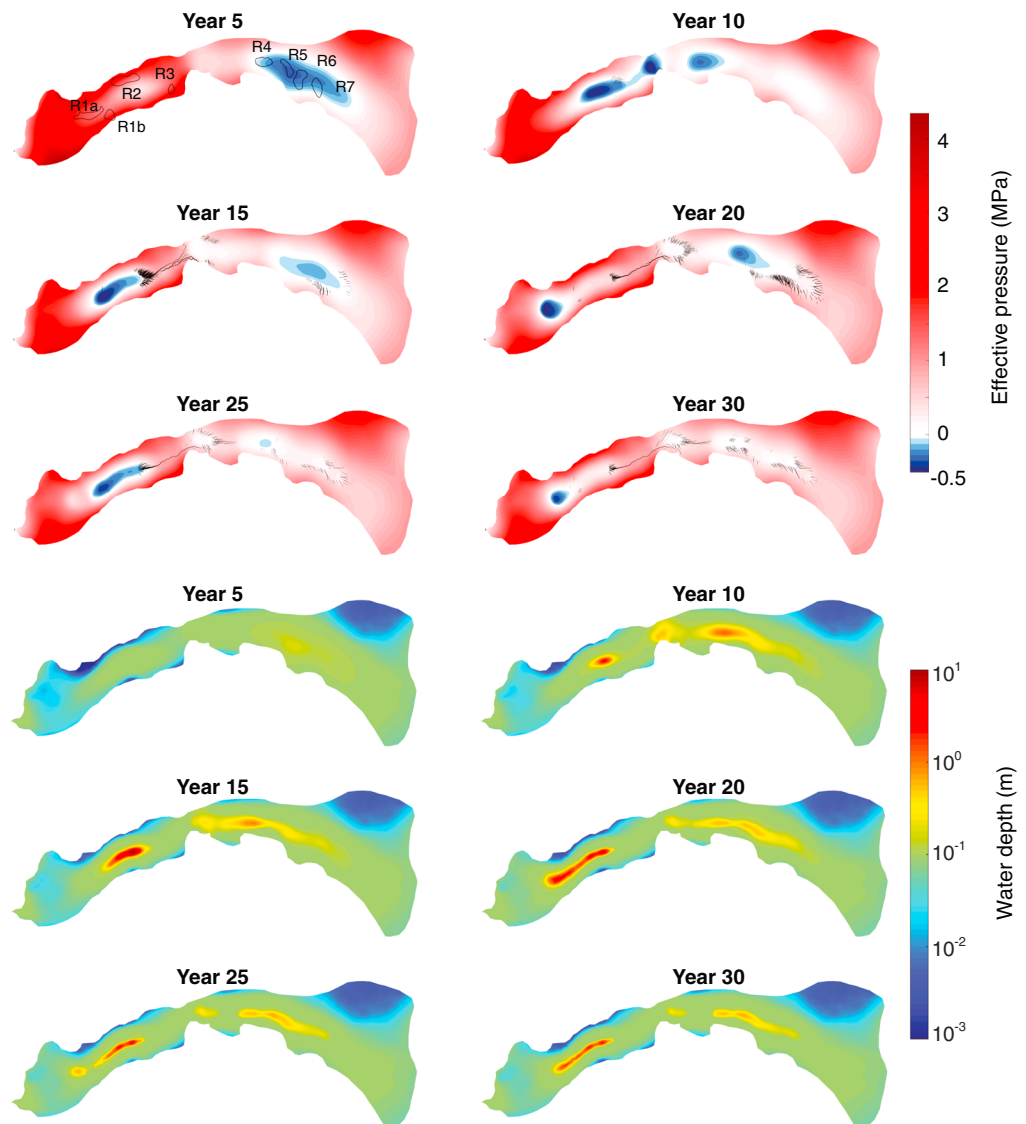
Figure 3. Effective pressure (including channel size shown by the black lines, with thicker lines indicating larger channels) and water depth outputs for the Recovery Ice Stream domain plotted at 5-year intervals.

that the large catchment draining into a narrow ice stream caused the formation of pressure waves. The subglacial drainage capacity of the ice stream was insufficient to remove the water supplied from the catchment, and so water pressure built up at the neck of the ice stream. This buildup locally increased the hydraulic potential gradient, causing faster water flow and the development of temporary channels that moved the water downstream. As the ice stream was constricted along its length, water that moved downstream once more could not be removed efficiently and so the water pressure again built up. This resulted in a transient pressure wave that moved through the ice stream. It was found in Dow et al. (2016) that, without these pressure waves, with a system in steady state, lake growth and drainage did not occur. With the pressure waves, the potential gradients along the drainage system were constantly altered and so steady state could not be achieved, thus allowing lake growth and drainage. In the synthetic system, these pressure waves, along with transient development of the hydrological network (such as growth of channels downstream of the lakes), were key drivers of the timing and extent of lake growth and drainage.

Pressure waves have been reported elsewhere in the literature, primarily associated with constricted subglacial regions where water is added more rapidly than hydrological network development can adapt to the volumes. A high-pressure wave of water was initiated by the 1996 Grímsvötn jökulhlaup in Iceland; this achieved pressures 5–10 bars above overburden but only persisted for 10 hr until the wave reached
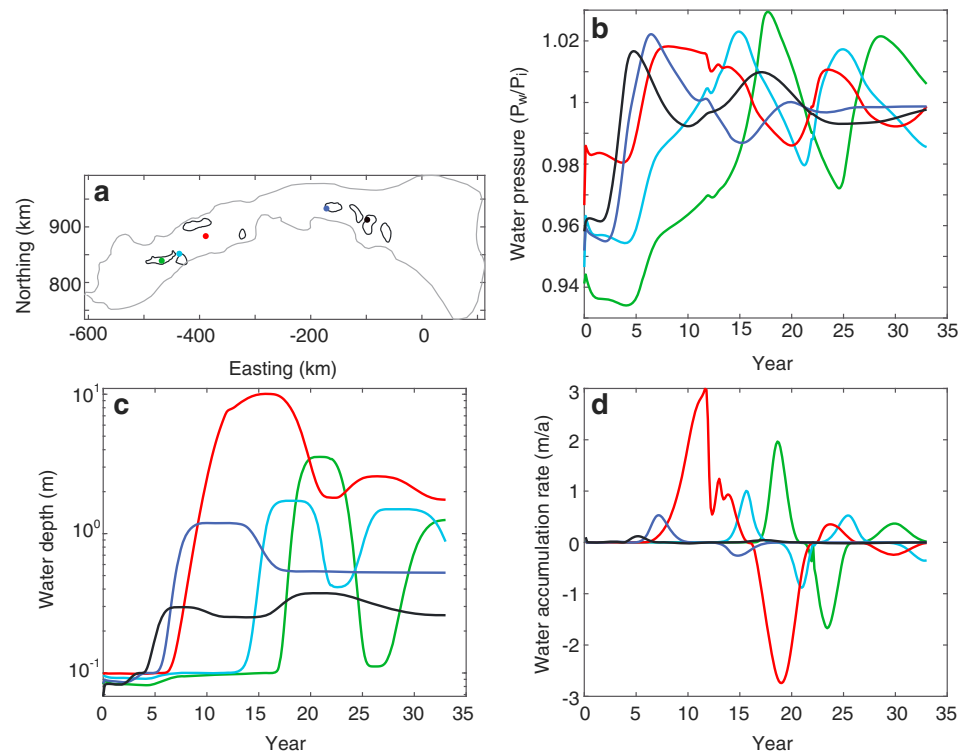
Figure 4. (a) Location of modeled outputs in Recovery Ice Stream plotted in (b)–(d). (b) Water pressure outputs plotted as a percentage of ice overburden. (c) Water depth outputs. (d) Water accumulation (positive) and drainage (negative) rates.

the glacier terminus (Johannesson, 2002). Other examples of pressure waves include data from constricted winter hydrological systems (Lingle & Fatland, 2003; Schoof et al., 2014), surging glaciers (Fatland & Lingle, 2002), and model outputs examining Greenland subglacial development in response to seasonal moulin and surface lake drainage inputs (Banwell et al., 2016).

In Dow et al. (2016), it was not clear whether applying more realistic topography to the modeled system would hinder this pressure wave development. However, we find that a similar phenomenon occurs with our current Recovery runs (Figure 3, plotted as effective pressure, i.e., ice pressure − water pressure). Due to the overdeepened trough in the middle of the ice stream (Figure 1), the lowest effective pressure (i.e., above overburden pressure) regions are more restricted to the ice stream center than found with the planar synthetic system in Dow et al. (2016). Despite this, in the current Recovery system, as the pressure wave passes, the full width of the ice stream is brought to overburden pressure. The first pressure wave causes widespread negative effective pressure. However, the drainage of the lakes drives the formation of channels, which persist during the passage of the second pressure wave and prevent the system reaching such extensive negative effective pressures as during the first wave.

As also found in the synthetic system, in both the steady state spin-up run and the standard runs where pressure waves form and propagate through the ice stream, water is never fully prevented from flowing out of the overdeepened regions. This is due to the coupled configuration of the hydrological model. Enough water flows out of the overdeepening in the distributed sheet to allow growth of small channels. These channels create a positive gradient between the lower effective pressure water in the lake basin and the slightly higher effective pressure network at the tip of the overdeepening.

The pressure waves are variable in extent and significance. The first pressure wave to move through the Recovery Ice Stream takes 17 years to fully propagate to within 100 km of the terminus where it then dissipates. However, during this time, an additional pressure wave forms at the head of the ice stream and propagates through, eventually catching up with the original pressure wave. This is a difference between the synthetic

system and the current configuration; in the synthetic model the pressure waves did not converge, suggesting that the variable topography of Recovery Ice Stream has a strong impact on the rate of downstream pressure wave transience.

3.3. Lake Depth and Water Pressure

Figure 2 shows the minimum effective pressure and maximum water thickness obtained from each element for the entire model run. R1a, R2, and R4 have the lowest effective pressure and deepest lakes of the model run (although not simultaneously). The narrow region of the ice stream between R3 and R4 also demonstrates negative effective pressure and water depths that fit into our lake classification scheme.

The deepest lake is R2 with a maximum depth of 10 m and R7 the shallowest, only gaining a maximum depth of 25 cm. The lake water depths are plotted in Figure 4c. Some lakes are shallower during the second cycle, such as R2 which reaches a depth of only 2.6 m following the first drainage. In contrast, R1b has approximately the same lake depth in both cycles, while R5 and R6 have a greater depth in the second cycle. This illustrates the temporal variability in the lake characteristics that is dependent on the level of development of the remainder of the ice stream hydrological network. Such temporal variability in lake depth was also demonstrated in the synthetic lake (see Figure 6a: Dow et al., 2016), with no discernible pattern or repetition over 100 years of model run time.

As the lakes grow and drain, the pressure within the lakes temporarily exceeds overburden pressure, similar to the synthetic lake. The maximum pressure obtained in the current model is 103% of overburden by R1a. This region persists above overburden for 4.6 years. The pressure range of the lakes ranges between 97% and 102% of overburden and lasts above overburden for ~5 years; these model outputs are plotted in Figure 4b.

The first drainage cycle has a cascading pattern with R7, R6 and R5 growing almost simultaneously. This is followed by growth of the rest of the lakes in a downstream sequence. However, by the time R1a (the lowest lake) is draining, the upper lakes have filled and drained again and the spatial drainage pattern becomes more complex. Such complexity is also visible in the ice elevation data as discussed below, although did not occur with the synthetic model runs, which only had one lake (see Figure 4: Dow et al., 2016).

3.4. Channels

The largest channels in the domain grow due to the lake drainage events (Figure 3). In particular, the drainage between Lakes R4 and R2 creates a large channel with a cross-sectional area up to 14 m^2. This is temporary and the channel reduces in size to 2.4 m^2 following the cessation of the first upper ice stream drainage cycle. During passage of the next pressure wave, a second channel grows parallel to the first and poaches water causing the first channel to shut down and the second to widen to a cross-sectional area of 21 m^2. Following passage of the second drainage cycle, this channel reduces to a size of 12 m^2.

Between 200 and 400 km from the ice stream terminus, channels play a large role in moving water from lake to lake. In contrast, the lakes in the upper and lower regions of the ice stream are located relatively close together in troughs and so channels do not form between these basins. Similarly, in the region 100 km from the terminus, channels do not grow into a network and drainage is instead dominated by the distributed drainage system.

3.5. Sensitivity Tests

We tested the sensitivity of the model outputs by altering several parameters individually and running from steady state. As the hydrological system is influenced by drainage development over the entire ice stream, the change of parameter has spatially and temporally variable impacts. To compare the model sensitivity results, we examine the outputs for R4 (blue point in Figure 4a). For each of these tests, the minimum effective pressure values did vary but were within 1% of the baseline pressure.

Lowering the sheet conductivity from 1×10^{-3} m$^{7/4}$ · kg$^{-1/2}$ to 9×10^{-4} m$^{7/4}$ · kg$^{-1/2}$ causes a lake 14% deeper than the baseline run (this is the deepest lake in the sensitivity tests). The first pressure wave has similar timing, but the second pressure wave transitions earlier by ~200 days. A higher sheet conductivity of 1.1×10^{-3} m$^{7/4}$ · kg$^{-1/2}$ causes the opposite phenomenon with lake depth 12% lower than the baseline and slower pressure wave formation lagging the baseline by ~400 days.

The water input rate into the ice stream upper boundary is calculated from the full catchment flux model run and varies across the boundary. The average rate is ~1×10^{-4} m^2/s. To test the impact of the boundary flux, we apply a spatially fixed, lower rate of water input of 8×10^{-5} m^2/s. With this input, the R4 lake is 60% smaller
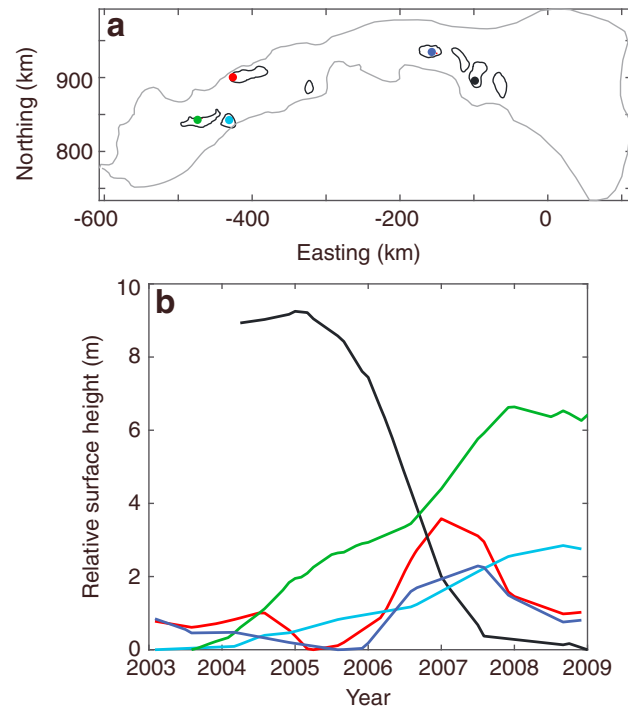
Figure 5. (a) Location of ICESat elevation time series on Recovery Ice Stream plotted in (b). (b) Observed ice sheet surface elevation time series derived from altimetry over the Recovery lakes.

than the baseline (the shallowest lake in the sensitivity tests). The initial pressure wave moves through the system much more slowly, peaking ~4.5 years after the baseline. A higher spatially fixed boundary water input of 1.2×10^{-4} m^2/s still causes a shallower lake than the baseline by 14%. However, the pressure wave peaks ~50 days before the baseline.

A lower channel conductivity of 1×10^{-2} m$^{3/4} \cdot$ kg$^{-1/2}$ (compared to the baseline of 5×10^{-2} m$^{3/4} \cdot$ kg$^{-1/2}$) causes a lake 33% shallower than the baseline and a slower second pressure wave that does not peak until ~5 years following the baseline peak. In this test, the lake takes twice as long to drain as the baseline lake (8 versus 4 years). Higher channel conductivity of 7×10^{-2} m$^{3/4} \cdot$ kg$^{-1/2}$ causes a lake depth very similar to the low channel conductivity run. However, the pressure wave does peak much earlier, 300 days following the baseline effective pressure.

Reducing the bedrock bump height in the model impacts the cavity opening rate as, once the cavities are flooded (i.e., the water depth is greater than this value), the sheet thickens only due to changing water pressure. The baseline bedrock bump height is 0.1 m. If this is lowered to 0.08 m, the lakes form ~2 years earlier and 9% deeper than the baseline. The second pressure wave occurs 3.3 years earlier and, in this model run, a third pressure wave forms and begins to propagate downstream.

3.6. Ice Sheet Elevation Observations

Ice sheet elevation time series derived from ICESat laser altimetry using SERAC are shown in Figure 5. These data span 6 years from 2003 to 2009. The lowest lake in the elevation data set is R1a. In this region the ice uplifts by 3 m over 2.5 years at the same time that R2 is draining. At this stage (2.5 years), R6 begins to drain, with substantial ice surface lowering of 9 m in 2 years. By year 4, R2 has filled again and begins to drain again. Between year 2.5 and 4, R1a has continued to uplift at around the same rate as the initial 2.5 years. After this, the rate of growth increases, likely in response to the drainage of R2. If we compare this to the model outputs, it appears that the initial 2.5 years is capturing the end of a pressure wave/drainage event through the ice stream while pressure builds up at the head of the ice stream. A second drainage event then initiated from R6 and moves through R2 to R1. R1 therefore grows as a result of two drainage events through the ice stream. Such complexity with some altimetry lakes growing throughout two drainage cycles (R1) while others have two cycles (R2) can also be seen in the modeled outputs. For example, in the model, R6 grows and drains twice in the period that R1 grows and drains (compare Figures 4b, 4c, and 5b).

4. Discussion

We begin by discussing the general model outputs before examining the lake characteristics, the role of channels, and what the model outputs suggest about the impact of the hydrological system on ice dynamics.

The subglacial drainage features (including the pressure waves and channel development patterns) that occur in the modeled Recovery Ice Stream are similar to those seen with the synthetic (simplified planar) system (Dow et al., 2016) but are more topographically constrained by the large trough in the middle of the ice stream (Figure 1). In the synthetic system, passage of pressure waves caused a small (centimeter-scale), temporary (~2 years) increase in water thickness at the base in regions where there was no lake. In the current, more realistic topography, the pressure waves and related water thickness changes are restricted to the troughs in the ice stream center and also downstream of R1 (compare Figure 3 and Figure 5 in Dow et al., 2016). Given the limited water thickness change outside of the lake basins in the more realistic model, it is unlikely that passage of a pressure wave would be visible in satellite altimetry data. However, it is possible that pressure waves in Recovery Ice Stream (and potentially other hydrologically restricted systems) could be identified in satellite horizontal velocity data products due to the high, sustained water pressures.

4.1. Lakes

Previous analyses of subglacial lake dynamics have assumed that their growth and drainage is a function of the volume of water accumulated in the lake until either ice over the lip of the overdeepening is uplifted sufficiently to allow downstream water flow (Ng & Liu, 2009; Nye, 1976), or a negative pressure gradient downstream of the lake is reversed due to hydrological network development (Fowler, 1999). Both theories have previously been applied to Icelandic jökulhlaup dynamics (e.g., Clarke, 1982; Nye, 1976).

In contrast, from our modeling exercise and from our synthetic model runs (Dow et al., 2016), we find that there is never a negative hydraulic gradient preventing water flow out of the overdeepening. Instead, lake growth and drainage is driven by the change in hydraulic potential within the ice stream, which is influenced by the passage of pressure waves. As a result, rates of lake growth and drainage and resulting lake depths are not identical every cycle. In our current model runs, we are restricted to 33 years as a result of computational limitations. We therefore do not know whether the lake filling and drainage cycles continue past the two cycles we show here. However, the synthetic model, which had similar inputs, albeit with a planar topography, demonstrated continued lake growth and drainage (and pressure wave transience) over 100 years. In these synthetic model runs, no two lake growth and drainage cycles were identical or repeated. We postulate that a similar phenomenon would occur with our current model runs if we could extend them to 100 years.

The changes in lake depth, channel size, and pressure in each drainage cycle, in both the current and synthetic model, suggest that with a 2-D coupled efficient and inefficient drainage network, it is not merely the local conditions that impact drainage development, but the entire ice stream. For example, in the current model runs, with an efficient channel developing between lakes in the middle region of the ice stream, the potential gradients become steeper and translate upglacier. Therefore, water reaccumulating in lakes upstream will flow more rapidly out of the overdeepenings and the upper lakes will drain sooner than they do when no large channel is present downstream. This suggests both a highly variable nature of the subglacial drainage systems in the Antarctic and also that local (tens of kilometers) drainage development is translated over a long distance (hundreds of kilometers) and can have impacts on the hydrological system (and by proxy, the ice dynamics) of the entire ice stream.

In both the current and the synthetic model runs, the highest water pressure in the lakes does not occur at the same time as the greatest depth in the lakes (Figures 4b, and 4c; Figure 6 in Dow et al., 2016). Instead, it is the *rate* of lake growth and drainage that closely follows the changes in water pressure. As the rate of water buildup in the lake increases, the pressure also increases. Water is continually flowing out of the lake overdeepening and with the pressure buildup, the resulting hydraulic potential increase drives more water downstream. Greater water flux eventually creates a more efficient system by developing channels at the lip of the overdeepening and water can then be evacuated more rapidly from the lake. At this stage the water pressure in the lake begins to drop and the rate of lake growth also drops. However, the absolute volume of water in the lake may still be increasing.

When comparing the observed ice sheet elevation time series with our model outputs, we have not fully replicated the drainage system between the years 2003 and 2009. We find that the depths of water accumulated in our modeled lakes are different than the surface elevation changes identified in the same regions although,

as shown in our sensitivity tests, this is somewhat dependent on parameter choice. For example, our maximum R1a depth is 4 m and in the ice altimetry data the maximum elevation change is ∼6.5 m. In contrast, our R2 maximum depth is 10 m and in the ice elevation data is 4 m. The largest discrepancy is between the modeled R6 depth of 0.4 m compared to ice elevation data of 9 m. As noted above, each modeled pressure wave and lake drainage event has different characteristics dependent on the previous pressure wave/lake drainage. We are therefore limited by only having part of one full drainage cycle observed in the Recovery region due to lack of satellite data, and by the length of our model run. This will improve with future data collection campaigns.

Other limitations for running the model include imperfect topographical data, estimated basal water inputs, and a lack of knowledge about basal conditions such as spatially variable conductivity and bed material. The model application is also limited in that it does not include ice flexure or dynamics, which may impact the lake drainage characteristics (Pattyn, 2008; Sergienko et al., 2007). These model limitations are discussed in greater detail by Dow et al. (2016). It is possible that by incorporating flexure and dynamics, our modeled negative effective pressure would diminish toward overburden. We will be exploring this with future modeling work. With this study, we therefore aim to illuminate major characteristics of the subglacial drainage development and variability of this ice stream to encourage further study and greater data collection.

4.2. Channels

It has been suggested by Carter et al. (2017) that it is not possible to have lake growth and drainage partially controlled by R-channel development as opposed to canals carved into underlying sediment. We demonstrate both here (and in the synthetic model, Dow et al., 2016) that it is indeed possible to have lake drainage related to R-channel growth. Large R-channels in the current system develop as a result of lake drainage and serve to rapidly translate water downstream toward other lakes. This is particularly obvious between the −300 and −350 km Easting region (Figure 3). Here the channel grows to 21 m^2 with a discharge of 11 m^3/s.

The role of the channels in Recovery Ice Stream is primarily for rapid water translation. They do limit the amount of low effective pressure in that they remove enough water to keep pressures just below overburden. However, these sizeable channels do not increase the effective pressure in the ice stream to a similar extent as those found in Alpine or Greenlandic systems (e.g., Bartholomew et al., 2012; Iken & Bindschadler, 1986). This is largely because of the shallow surface slopes of the ice stream preventing a strong hydraulic potential gradient. The constricted nature (low potential gradient and low hydrologic conductivity) of the ice stream and the lack of seasonality in the drainage system also prevent the highly efficient channels that are found in mountain glaciers. In Recovery Ice Stream, the channels are present due to the constant water supply from the lakes, and once those lakes drain, the reduced water availability cause the channels to close. Thus, the channels do have a role in ice stream drainage development, but because they do not greatly increase the system effective pressure, likely do not have a large impact on ice flow speed.

We have evidence of channel evolution during lake drainage. Between −300 and −350 km Easting there are initially three smaller (<14 m^2) channels running parallel to each other that, over the period of 4.5 years, merge into one larger (21 m^2) channel. The location of the larger channel is likely to be pervasive for most lake drainage events. As a result this is a location where there may be bedrock or sediment scouring, creating a larger channel. Given that the topographical data have enough uncertainty that our modeled lakes do not overlap perfectly with the observed lakes, it is unclear whether a bedrock channel exists in the location suggested by the model. However, the model outputs suggest that large channels are possible in Recovery Ice Stream, and with improved topography data in the future, could predict where basal channels will be present.

4.3. Ice Dynamics

The negative effective water pressures caused by passage of the pressure wave should have an impact on ice velocity with faster ice flow speeds occurring in the low effective pressure areas. We compare the minimum effective pressure in each model element with the MEaSUREs ice velocity data set (Figures 2a and 2c), which is a composite from multiple years of satellite data (Rignot et al., 2011). We find that there are consistent patterns between the model pressure outputs and the velocity data set. The regions where ice speeds are >80 m/a are similar to the regions where water pressures exceed overburden in the model. This includes a region 300 km from the ice front where there is a strong modeled pressure signal coincident with high measured ice surface velocity, where a lake was not previously identified from ICESat altimetry data. Farther downstream, the ice rapidly speeds up in the region of R1a/R1b and R2 where we see low effective pressure in the model. Closer to the terminus, the ice stream speed increases further but is not consistent with our regions of low effective

pressure. Perhaps in this region, within 100 km of the grounding line, there are wet and deformable marine sediments, which we do not take into account with this model.

The overlap between regions of fast ice surface velocity and low basal effective water pressure suggest that the concentration of water in the central trough could play an important role in maintaining the speed of Recovery Ice Stream. The consistency is greater between ice velocity and the basal water pressure rather than the depth of the water within the lakes. This suggests that the water pressure plays a more important role in the ice stream velocity than the water thickness, which as we demonstrate with our model outputs is not always coincident with water pressure, either spatially or temporally.

5. Summary

We have modeled the evolution of Recovery Ice Stream basal hydrological system using a 2-D subglacial hydrology model. Our model outputs demonstrate growth and drainage of lakes that match well with most of the Recovery lakes identifiable from ice surface laser altimetry data, which are available from 2003 to 2009. An encouraging result is the good overlap between the regions with lowest effective pressure and fast ice surface speed in Recovery Ice Stream that suggest the areas where lakes are accumulating and draining in the model have a strong impact on the dynamics of the ice stream.

Recovery Ice Stream has previously been modeled as a synthetic system with one overdeepening (Dow et al., 2016) and the outputs from the current configuration applied to real topography are similar to the synthetic system in several ways. Both model setups produce pressure waves that propagate through the ice stream. These transient features are caused by constriction at the ice stream neck where relatively large quantities of subglacial water enter from the substantial drainage catchment. Low effective pressures are focused in the center of the ice stream where there is a large trough with multiple overdeepenings. The pressure waves cause a continual change in subglacial hydraulic potential, which contributes to the growth and drainage of the subglacial lakes; in the steady state scenario, no water accumulates in the lake basin. Once pressures increase in the lake basin, they cause steeper potential gradients that drive more water downstream. This water allows growth of channels at the lip of the overdeepening and, once these have sufficiently developed, the lake drains, moving the water downstream into the next lake basin in a cascading pattern. At no point is water fully prevented from leaving the overdeepening, suggesting that these lakes can be considered as transient regions of the drainage system rather than impounded bodies of water. In both systems we also find that the larger-scale extent of hydrological development of the ice stream is important for determining the timing of lake growth and drainage, with a more hydrologically efficient system preventing larger lakes forming. This means that the lake size and drainage timing are not identically repeated with every pressure wave.

The current model applied to real topography makes advances beyond the synthetic configuration. We ran the model for 33 years and found that multiple pressure waves propagate through the ice stream. A primary finding is that the rate of pressure wave passage through Recovery Ice Stream is variable with the deep troughs of the lower lakes slowing the pressure wave transit. This results in multiple pressure waves moving through the ice stream at the same time, complicating the cascading pattern of lake growth and drainage from upstream to downstream. We also find that the drainage of large volumes of water can cause channels to develop between the lakes. These channels persist for multiple years until the water supply from the lake is diminished, after which the channels shrink but do not disappear entirely. These channels act to rapidly move water between lake basins. However, we do not see any channels in the terminal 100 km of the ice stream, or low effective water pressures, both of which may be a result of limited basal topography data to use as model inputs. Finally, due to the deep nature of the Recovery Ice Stream basal trough, both the highest water pressures and drainage routes are focused here, perhaps influencing the flow speed of the ice stream. These findings have implications for interpreting satellite altimetry data over Antarctic subglacial lakes, establishing spatial and temporal variability of drainage networks underneath ice streams and determining controls of hydrology on ice dynamics.

The outputs from GlaDS subglacial hydrology model that we have discussed raise interesting questions about subglacial hydrological development of Antarctic systems and the role that lakes play in ice dynamics. Future work will include linking the basal hydrology model with ice dynamics. Larger volumes of data from future airborne and satellite missions will also aid the application of this model.

References

Banwell, A., Hewitt, I., Willis, I., & Arnold, N. (2016). Moulin density controls drainage development beneath the Greenland ice sheet. *Journal of Geophysical Research: Earth Surface*, *121*, 2248–2269. https://doi.org/10.1002/2015JF00380

Bartholomew, I., Nienow, P., Sole, A., Mair, D., Cowton, T., & King, M. A. (2012). Short-term variability in Greenland ice sheet motion forced by time-varying meltwater drainage: Implications for the relationship between subglacial drainage system behavior and ice velocity. *Journal of Geophysical Research*, *117*, F03002. https://doi.org/10.1029/2011JF002220

Bell, R. E., Studinger, M., Shuman, C. A., Fahnestock, M. A., & Joughin, I. (2007). Large subglacial lakes in East Antarctica at the onset of fast-flowing ice streams. *Nature*, *445*(7130), 904–907.

Borsa, A. A., Moholdt, G., Fricker, H. A., & Brunt, K. M. (2014). A range correction for ICESat and its potential impact on ice-sheet mass balance studies. *The Cryosphere*, *8*(2), 345–357. https://doi.org/10.5194/tc-8-345-2014

Carter, S., & Fricker, H. (2012). The supply of subglacial meltwater to the grounding line of the Siple Coast, West Antarctica. *Annals of Glaciology*, *53*(60), 267–280.

Carter, S. P., Blankenship, D. D., Young, D. A., Peters, M. E., Holt, J. W., & Siegert, M. J. (2009). Dynamic distributed drainage implied by the flow evolution of the 1996–1998 Adventure Trench subglacial lake discharge. *Earth and Planetary Science Letters*, *283*(1), 24–37.

Carter, S. P., Fricker, H. A., Blankenship, D. D., Johnson, J. V., Lipscomb, W. H., Price, S. F., & Young, D. A. (2011). Modeling 5 years of subglacial lake activity in the MacAyeal Ice Stream (Antarctica) catchment through assimilation of ICESat laser altimetry. *Journal of Glaciology*, *57*(206), 1098–1112.

Carter, S. P., Fricker, H. A., & Siegfried, M. R. (2017). Antarctic subglacial lakes drain through sediment-floored canals: Theory and model testing on real and idealized domains. *The Cryosphere*, *11*(1), 381–405.

Clarke, G. K. C. (1982). Glacier outburst floods from 'Hazard Lake' Yukon Territory, and the problem of flood magnitude prediction. *Journal of Glaciology*, *28*(98), 3–21.

Creyts, T. T., & Schoof, C. G. (2009). Drainage through subglacial water sheets. *Journal of Geophysical Research*, *114*, F04008. https://doi.org/10.1029/2008JF001215

Dow, C. F., Werder, M. A., & Walker, R. T. (2016). Modeling Antarctic subglacial lake filling and drainage cycles. *The Cryosphere*, *10*(4), 1381–1393.

Evatt, G., Fowler, A., Clark, C., & Hulton, N. (2006). Subglacial floods beneath ice sheets. *Philosophical Transactions of the Royal Society of London A: Mathematical, Physical and Engineering Sciences*, *364*(1844), 1769–1794.

Fatland, D. R., & Lingle, C. S. (2002). Insar observations of the 1993–95 Bering Glacier (Alaska, USA) surge and a surge hypothesis. *Journal of Glaciology*, *48*(162), 439–451.

Fowler, A. (1999). Breaking the seal at Grímsvötn, Iceland. *Journal of Glaciology*, *45*(151), 506–516.

Fretwell, P., Pritchard, H. D., Vaughan, D. G., Bamber, J., Barrand, N., Bell, R., et al. (2013). Bedmap2: Improved ice bed, surface and thickness datasets for Antarctica. *The Cryosphere*, *7*(1), 375–393.

Fricker, H. A., Borsa, A., Minster, B., Carabajal, C., Quinn, K., & Bills, B. (2005). Assessment of ICESat performance at the Salar de Uyuni, Bolivia. *Geophysical Research Letters*, *32*, L21S06. https://doi.org/10.1029/2005GL023423

Fricker, H. A., Carter, S. P., Bell, R. E., & Scambos, T. (2014). Active lakes of Recovery Ice Stream, East Antarctica: A bedrock-controlled subglacial hydrological system. *Journal of Glaciology*, *60*(223), 1015–1030.

Fricker, H. A., Scambos, T., Carter, S., Davis, C., Haran, T., & Joughin, I. (2010). Synthesizing multiple remote-sensing techniques for subglacial hydrologic mapping: Application to a lake system beneath Macayeal Ice Stream, West Antarctica. *Journal of Glaciology*, *56*(196), 187–199.

Fricker, H. A., Siegfried, M. R., Carter, S. P., & Scambos, T. A. (2016). A decade of progress in observing and modelling Antarctic subglacial water systems. *Philosophical Transactions of the Royal Society A: Mathematical, Physical and Engineering Sciences*, *374*(2059), 20140294.

Iken, A., & Bindschadler, R. A. (1986). Combined measurements of subglacial water pressure and surface velocity of Findelengletscher, Switzerland: Conclusions about drainage system and sliding mechanism. *Journal of Glaciology*, *32*(110), 101–119.

Johannesson, T. (2002). Propagation of a subglacial flood wave during the initiation of a jökulhlaup. *Hydrological Sciences Journal*, *47*(3), 417–434.

Joughin, I., Bamber, J. L., Scambos, T., Tulaczyk, S., Fahnestock, M., & MacAyeal, D. R. (2006). Integrating satellite observations with modelling: Basal shear stress of the Filcher-Ronne ice streams, Antarctica. *Philosophical Transactions of the Royal Society of London A: Mathematical, Physical and Engineering Sciences*, *364*(1844), 1795–1814.

Joughin, I., Tulaczyk, S., Bindschadler, R., & Price, S. F. (2002). Changes in West Antarctic ice stream velocities: Observation and analysis. *Journal of Geophysical Research*, *107*(B11), 2289. https://doi.org/10.1029/2001JB001029

Kingslake, J. (2015). Chaotic dynamics of a glaciohydraulic model. *Journal of Glaciology*, *61*(227), 493–502.

Langley, K., Kohler, J., Matsuoka, K., Sinisalo, A., Scambos, T., Neumann, T., et al. (2011). Recovery Lakes, East Antarctica: Radar assessment of sub-glacial water extent. *Geophysical Research Letters*, *38*, L05501. https://doi.org/10.1029/2010GL046094

Langley, K., Tinto, K., Block, A., Bell, R., Kohler, J., & Scambos, T. (2014). Onset of fast ice flow in Recovery Ice Stream, East Antarctica: A comparison of potential causes. *Journal of Glaciology*, *60*(223), 1007–1014.

Lingle, C. S., & Fatland, D. R. (2003). Does englacial water storage drive temperate glacier surges? *Annals of Glaciology*, *36*(1), 14–20.

Morlighem, M., Rignot, E., Seroussi, H., Larour, E., Ben Dhia, H., & Aubry, D. (2011). A mass conservation approach for mapping glacier ice thickness. *Geophysical Research Letters*, *38*, L19503. https://doi.org/10.1029/2011GL048659

Ng, F., & Liu, S. (2009). Temporal dynamics of a jökulhlaup system. *Journal of Glaciology*, *55*(192), 651–665.

Nye, J. F. (1976). Water flow in glaciers: jökulhlaups, tunnels and veins. *Journal of Glaciology*, *17*(76), 181–207.

Pattyn, F. (2008). Investigating the stability of subglacial lakes with a full Stokes ice-sheet model. *Journal of Glaciology*, *54*(185), 353–361.

Rignot, E., Mouginot, J., & Scheuchl, B. (2011). Ice flow of the Antarctic ice sheet. *Science*, *333*(6048), 1427–1430.

Schenk, T., & Csatho, B. (2012). A new methodology for detecting ice sheet surface elevation changes from laser altimetry data. *IEEE Transactions on Geoscience and Remote Sensing*, *50*(9), 3302–3316.

Schoof, C., Rada, C., Wilson, N., Flowers, G., & Haseloff, M. (2014). Oscillatory subglacial drainage in the absence of surface melt. *The Cryosphere*, *8*(3), 959–976.

Sergienko, O., MacAyeal, D., & Bindschadler, R. (2007). Causes of sudden, short-term changes in ice-stream surface elevation. *Geophysical Research Letters*, *34*, L22503. https://doi.org/10.1029/2007GL031775

Siegert, M. J. (2005). Lakes beneath the ice sheet: The occurrence, analysis, and future exploration of Lake Vostok and other Antarctic subglacial lakes. *Annual Review of Earth and Planetary Sciences*, *33*, 215–245.

Siegfried, M. R., Fricker, H. A., Carter, S. P., & Tulaczyk, S. (2016). Episodic ice velocity fluctuations triggered by a subglacial flood in West Antarctica. *Geophysical Research Letters*, *43*, 2640–2648. https://doi.org/10.1002/2016GL067758

Smith, B. E., Fricker, H. A., Joughin, I. R., & Tulaczyk, S. (2009). An inventory of active subglacial lakes in Antarctica detected by ICESat (2003–2008). *Journal of Glaciology*, *55*(192), 573–595.

Tulaczyk, S., Kamb, W. B., & Engelhardt, H. F. (2000). Basal mechanics of Ice Stream B, west Antarctica: 2. Undrained plastic bed model. *Journal of Geophysical Research*, *105*(B1), 483–494.

van Wessem, J. M., Reijmer, C. H., Morlighem, M., Mouginot, J., Rignot, E., Medley, B., et al. (2014). Improved representation of East Antarctic surface mass balance in a regional atmospheric climate model. *Journal of Glaciology*, *60*(222), 761–770. https://doi.org/10.3189/2014JoG14J051

Werder, M. A., Hewitt, I. J., Schoof, C. G., & Flowers, G. E. (2013). Modeling channelized and distributed subglacial drainage in two dimensions. *Journal of Geophysical Research: Earth Surface*, *118*, 2140–2158. https://doi.org/10.1002/jgrf.20146